Article

Selective Harmonic Elimination in a Cascaded Multilevel Inverter of Distributed Power Generators Using Water Cycle Algorithm

Muhammad Khizer [1], **Umar T. Shami** [2], **Muhammad Fahad Zia** [1], **Yassine Amirat** [3,*] **and Mohamed Benbouzid** [4,5]

[1] Department of Electrical Engineering, National University of Computer and Emerging Sciences, Lahore 54000, Pakistan; muhammadkhizeraltaf@outlook.com (M.K.); fahad.zia@nu.edu.pk (M.F.Z.)

[2] Department of Electrical Engineering, University of Engineering and Technology, Lahore 54000, Pakistan; utshami@uet.edu.pk

[3] ISEN Yncréa Ouest, L@bISEN, 29200 Brest, France

[4] Institut de Recherche Dupuy de Lôme (UMR CNRS 6027 IRDL), University of Brest, 29238 Brest, France; mohamed.benbouzid@univ-brest.fr

[5] Logistics Engineering College, Shanghai Maritime University, Shanghai 201306, China

* Correspondence: yassine.amirat@isen-ouest.yncrea.fr

Abstract: This research paper proposes the application of a meta-heuristic algorithm, namely the water cycle algorithm (WCA), for optimizing the performance of a multi-level inverter for a distributed energy resources-based smart grid system. The aim is to find the optimal switching angles to achieve selective harmonic elimination. To exhibit the effectiveness of the proposed algorithm and evaluate the results, a three-phase seven-level cascaded multilevel inverter (CHBMLI) is used. This paper demonstrates the efficacy of the proposed algorithm by performing a rigorous comparison with existing meta-heuristic algorithms. Independent sample *t*-tests for different population sizes are demonstrated, which reflect the better performance of the proposed algorithm's results. For the comparison, crucial parameters for optimization, including population size and number of iterations, are kept the same for the proposed WCA and other algorithms. Since we are solving a minimization problem, a lower fitness value is focused. In our research paper, we show how the proposed algorithm attains a lower fitness value and fast rate of convergence. For different values of the modulation index, WCA performs better than particle swarm optimization (PSO) and the firefly algorithm (FA). For a particular case of a modulation index value of 0.8, the minimum value found by WCA over 50 samples is 0.0001, whereas that of PSO and FA are 0.0223 and 0.0433, respectively, which shows that WCA has better accuracy. The results clearly present that the proposed algorithm provides a competitive percentage of elimination of selected harmonics when compared with other meta-heuristic algorithms.

Keywords: cascaded multilevel inverter; meta-heuristic optimization; renewable energy; selective harmonic elimination; water cycle algorithm

1. Introduction

Over the last few decades, multilevel inverters have found many industrial applications. They are being employed in medium voltage and high power electrical drives [1]. Multilevel inverters have also been extensively utilized in flexible AC transmission (FACT) and high voltage direct transmission (HVDC) based systems [2,3]. Multilevel inverters have three types: flying capacitor, diode clamped and cascaded H-bridge multilevel inverters (CHBMLI) [4–6]. Modularity and repetitive structure makes CHBMLI extensively used in renewable energy systems (RES) [7–9]. Additionally, CHBMLI has a fewer number of components. The employment of separate DC sources is also its desirable feature, especially

in PV systems [10,11]. Figure 1 presents an application of CHBMLI in a distributed energy resources-based power grid system. It consists of pre-defined H-bridge cells connected in series. Each cell has its independent DC power supply, and these power supplies can be the same or different. The number of levels obtained in a k-level CHBMLI is (2k + 1).
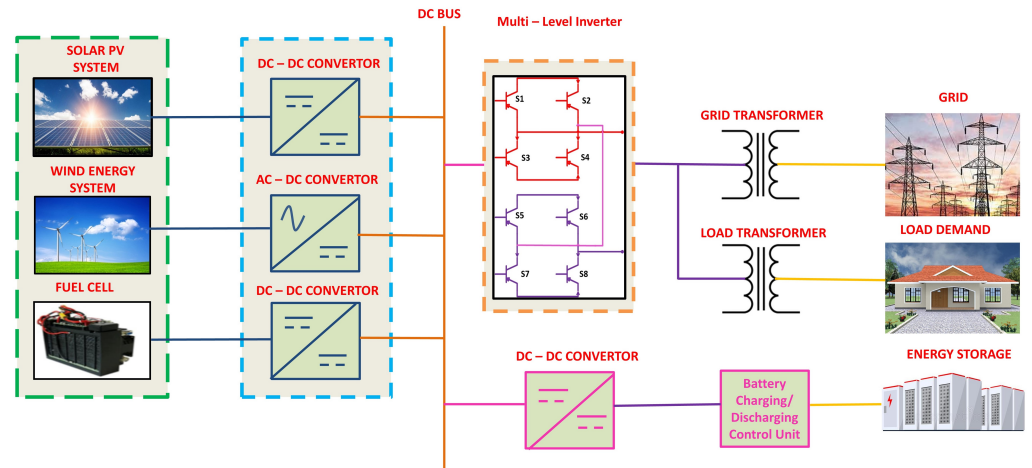

Figure 1. Multi-level inverter for distributed energy resources-based smart grid system.

Nowadays, a major challenge with a multilevel inverter (MLI) is focused on improving the power quality. For CHBMLI control, several modulation techniques exist in the literature. Conventional pulse width modulation (PWM), sinusoidal PWM, and space vector modulation are high-frequency switching techniques with a transient response. Furthermore, different carrier-based PWM techniques and carrier-less PWM techniques are introduced that effectively reduce distortion and reduce the electromagnetic interference (EMI). Inverter efficiency can be improved by the employment of low-pass filters of a high-order, which suppress high-order harmonics. However, dominant low-order harmonics, namely the third, fifth and seventh harmonics, cannot be eliminated completely using PWM-based switching techniques.

Selective harmonic elimination (SHE) is a low switching frequency technique. In SHE, switching angles are determined that eliminate the specific lower order harmonics while maintaining a fundamental order harmonic. These switching angles are determined by solving SHE equations. Various constraints need to be taken care of while determining switching angles using SHE equations. These include restricting angles between 0 and $\frac{\pi}{2}$ (assuming quarter-wave symmetry) and maintaining the fundamental to a defined value. The challenge associated while eliminating harmonics using the SHE technique is the solution to solve complex non-linear equations, as they contain trigonometric terms and exhibit a multi-modal nature.

Various methods have been discussed in the literature to solve SHE transcendental equations, which include numerical, algebraic methods, and bio-inspired methods [12]. In particular, numerical methods have been discussed in the literature to solve SHE equations. In [13], the application of Walsh functions for solving SHE equations is discussed. To solve SHE equations, the homotopy algorithm is applied in [14]. Sequential programming and Newton–Raphson methods are also discussed to solve SHE equations in [15,16], respectively. Although numerical methods give accurate solutions, they have a tendency to get trapped in local optima due to dependency on initial guess.

Algebraic methods, such as the resultant theory method [17], theory of Groebner bases [18], Wu method [19], symmetric polynomial [20], and power sum methods [21], have also been discussed in the literature to solve SHE complex nonlinear equations. Algebraic methods work by transforming non-linear algebraic equations into polynomial equations, and they do not require an initial guess. Hence, they are better as compared to numerical methods due to the non-requirement of an initial guess. However, these methods are only suitable for low-level inverters. With the increase in the number of inverter levels,

the complexity and computational burden of these methods also increase and they become unsuitable for real-time control of high-level power inverters.

In the past, many bio-inspired metaheuristic algorithms have been reported in the literature to solve SHE equations for CHBMLI. Early metaheuristic algorithms include the genetic algorithm (GA) and its variants [22]. GA is applied for the harmonic elimination of the 5th, 7th, and 11th harmonics in a three-phase nine-level inverter in [23], but the authors do not provide solutions for all values of the modulation index. Particle swarm optimization (PSO) is also applied to CHBMLI for SHE in [24]. In [25], the author presents the application of the bee algorithm (BA) to a 7-level inverter and compares its performance with GA. The author concludes that BA surpasses GA in the attainment of an accurate global minima, and the rate of convergence of BA is also better. In [26], the cuckoo search algorithm (CSA) is utilized for SHE in a 7-level CHBMLI. The author compares the performance of CSA with BA and GA and determines that CSA performs better than BA in eliminating selected harmonics, but the comparison in terms of convergence speed is not provided. The bat optimization algorithm (BOA) is applied to a three-phase 7-level CHBMLI for solving SHE equations [27], and the comparison of the reported algorithm is performed with GA and BA. The author reports the superiority of BOA over GA and BA in eliminating harmonics but does not compare the aforementioned techniques in terms of speed of convergence. In [28], employment of the firefly algorithm (FA) is reported for SHE in 11-level CHBMLI, having equal and unequal DC sources. The author suggests that FA performs better than PSO, GA, modified PSO, and NR, but a convergence comparison is not performed. Recently, many newly developed evolutionary algorithms have been applied for the SHE problem in CHBMLI [12]. The ant colony optimization (ACO) algorithm is applied to a three-phase 5-level inverter, and it is compared with GA in [29]. In [30], grey wolf optimizer (GWO) is reported for harmonic elimination in 11- and 15-level CHBMLIs, and its comparison is performed with PSO. It is reported that GWO outperforms PSO. In [31], the modified grey wolf optimizer (MGWO) is reported for the harmonic elimination problem in hybrid CHBMLI. In [32], a bacterial foraging algorithm is applied to solve SHE equations. The newly developed salt swarm algorithm (SSA) is also reported for the harmonic elimination problem in a 5-level inverter, and the author shows that SSA performs better than PSO in terms of convergence [33].

In the aforementioned papers, various algorithms have been applied to solve SHE equations for multilevel inverters. These algorithms require the tuning of multiple parameters for their optimal performance. This research proposes a state-of-the-art water cycle algorithm (WCA) for solving the SHE equations in a CHBMLI. WCA is simple to implement and requires the tuning of only one parameter for its optimal performance. The major contributions of this paper are as follows:

- Application of water cycle algorithm for solving selective harmonic equations of a cascaded H-bridge multi-level inverter.
- Comparison of computational complexity along with accuracy and speed of convergence with other meta-heuristic algorithms are provided to prove the effectiveness of the water cycle algorithm.
- Statistical comparison between different meta-heuristic algorithms using the independent sample *t*-test is also provided.

The remaining paper is organized as follows: Section 2 explains the problem formulation for CHBMLI; Section 3 illustrates the water cycle algorithm; Section 4 explains the simulation setup; Section 5 presents the results and analysis; and finally, Section 6 concludes the findings of the proposed work.

2. CHBMLI Problem Formulation

The SHE technique involves solving non-linear equations for CHBMLI. These equations are obtained by decomposing the waveform into its Fourier series. The even and cosine terms get zero due to the quarter wave symmetry due to the nature of the function being odd. Triplen harmonics also becomes canceled out in the line voltage.

For a M-Level three phase CHBMLI, having k cells, the degree of freedom is k, and $k - 1$ harmonics can be eliminated. The transcendental equations expressing the fundamental and dominant low order non-triplen harmonics for a CHBMLI can be formulated as given in Equations (1) and (2).

$$V_1 = \frac{4V_{dc}}{\pi}(cos(\psi_1) + cos(\psi_2) + cos(\psi_3)......cos(\psi_k)) \tag{1}$$

$$0 = \frac{4V_{dc}}{n\pi}(cos(n\psi_1) + cos(n\psi_2) + cos(n\psi_3)......cos(n\psi_k)) \tag{2}$$

The fundamental component can be expressed in terms of the modulation index (m_a) as given in Equation (3).

$$cos(\psi_1) + cos(\psi_2) + cos(\psi_3)......cos(\psi_k) = km_a = m \tag{3}$$

where,

$$m = \frac{V_1}{\frac{4V_{dc}}{\pi}} \tag{4}$$

$$m_a = \frac{V_1}{V_{max}} = \frac{V_1}{\frac{4kV_{dc}}{\pi}} = \frac{m}{k} \tag{5}$$

where V_1 is the fundamental value of the phase voltage obtained by the H-bridge. V_{max} is the maximum value of the phase voltage obtained by CHBMLI, and k is the number of H-bridge cells. V_{max} is obtained when all the switching angles are zero, i.e.,

$$V_{max} = \frac{4kV_{dc}}{\pi} \tag{6}$$

For a 7-level CHBMLI, the stepped waveform is shown in Figure 2. Following the illustration and modeling, SHE equations for a 7-Level CHBMLI can be formulated as follows:

$$cos(\psi_1) + cos(\psi_2) + cos(\psi_3) = 3m_a \tag{7}$$

$$cos(5\psi_1) + cos(5\psi_2) + cos(5\psi_3) = 0 \tag{8}$$

$$cos(7\psi_1) + cos(7\psi_2) + cos(7\psi_3) = 0 \tag{9}$$

Taking the cosine terms in Equation (7) to the right hand side, we obtain

$$3m_a - (cos(\psi_1) + cos(\psi_2) + cos(\psi_3)) = 0 \tag{10}$$

Since we are eliminating specific harmonics while maintaining the fundamental component to a particular value, we define an objective function which relates all the harmonics and the fundamental component. Taking this into consideration, an objective function is formulated, which is defined as the minimization function of the absolute sum of Equations (8)–(10), and it is given as below:

$$\begin{aligned} \text{Min } &|(3m_a - (cos(\psi_1) + cos(\psi_2) + cos(\psi_3)))| \\ &+ |(cos(5\psi_1) + cos(5\psi_2) + cos(5\psi_3))| \\ &+ |(cos(7\psi_1) + cos(7\psi_2) + cos(7\psi_3))| \end{aligned} \tag{11}$$

where the first term minimizes the error between the desired fundamental value defined by the modulation index and the obtained fundamental value, while the second and third terms minimize the 5th and 7th harmonics.
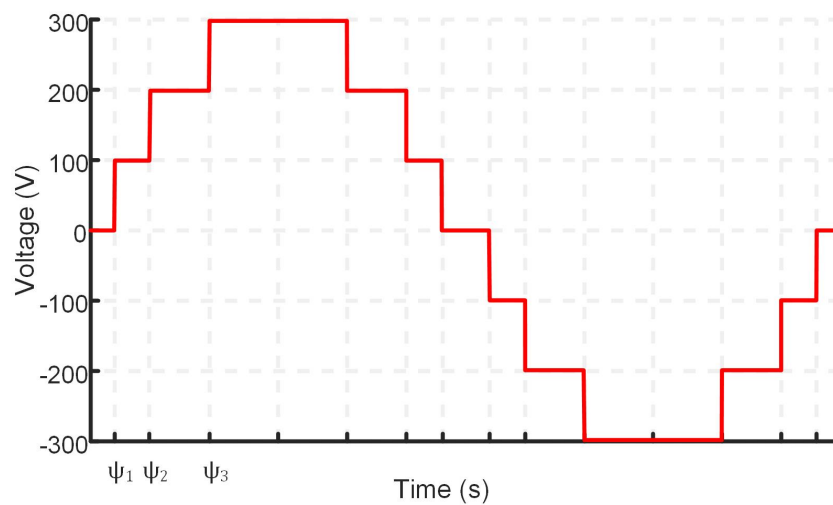
Figure 2. Stepped waveform for a 7-level inverter.

3. Water Cycle Algorithm

The water cycle is an evolutionary algorithm proposed by Ali Sadollah [34]. It is based on the natural water cycle and the downhill flow of rivers and streams toward the sea. In a natural water cycle, water is evaporated and clouds are formed through the process of condensation. After that, water comes down to earth through the process of rain. This water then takes the form of rivers and streams and is evaporated again, and this whole cycle is repeated. In WCA, solutions are termed as *'raindrops'*. Initially, the raining process is assumed. The raindrops that give the best and good fitness values are designated as *'sea'* and *'rivers'*, respectively. The rest of the solutions are designated as *'streams'*. According to the magnitude of flow, streams are absorbed by the rivers which eventually fall into the sea (the global best). The flowchart of WCA is illustrated by Figure 3. The steps of WCA are explained in the following subsections.

3.1. Generation of Initial Population

For initiation of the algorithm, the initial random population of the raindrops is generated. For an optimization problem with a number of variables N_{var}, the initial solution vector (raindrop) with dimensions $1 \times N_{var}$ is represented by Equation (12).

$$R_{1 \times N_{var}} = [r_1 \ r_2 \ r_3 \cdots \cdots \cdots r_{N_{var}}] \tag{12}$$

For a population size of N_{pop}, the initial solution matrix with dimensions $N_{pop} \times N_{var}$ is generated, and it is modeled in Equation (13).

$$R_{(N_{pop}, N_{var})} = \begin{pmatrix} r_{1,1} & r_{1,2} & \cdots & r_{1,N_{var}} \\ r_{2,1} & r_{2,2} & \cdots & r_{2,N_{var}} \\ \vdots & \vdots & \ddots & \vdots \\ r_{N_{pop},1} & r_{N_{pop},2} & \cdots & r_{N_{pop},N_{var}} \end{pmatrix} \tag{13}$$

3.2. Evaluation of Fitness Function

For each raindrop r, the fitness function value is evaluated by

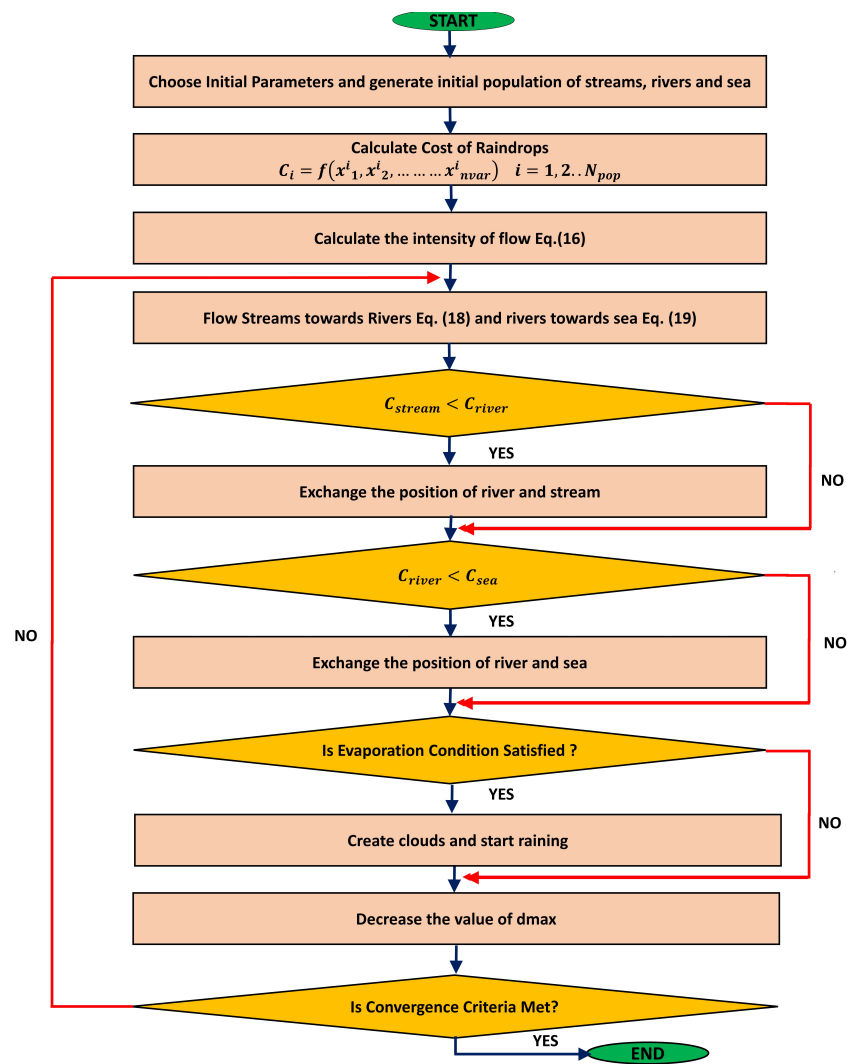$$FF_i = FF(r1, r2, r3, \cdots, rNvar) \tag{14}$$

Figure 3. Flowchart illustrating working of water cycle algorithm.

The number of rivers, denoted as *nr*, is chosen by the user. The rest of the raindrops are chosen as streams. The quantity N_{sr}, defined in Equation (15), is equal to the sum of the rivers and sea (1 represents sea).

$$N_{sr} = nr + 1 \tag{15}$$

The number of streams denoted by N_s is given using Equation (16).

$$N_s = N_{pop} - N_{sr} \tag{16}$$

3.3. Allocation of Streams to Rivers and Sea

Streams are allocated to respective rivers and sea based on their magnitude of flow given by Equation (17).

$$NS_i = round\left\{\left|\frac{Cost_i}{\sum_{n=1}^{N_{sr}} Cost_n}\right|\right\} \times N_s \tag{17}$$

where $i = 1, 2, \ldots, N_{sr}$. $Cost_i$ is the value of the objective function evaluated at specific rivers and the sea. NS_i is the number of streams, which move toward specific rivers and the sea.

3.4. Position Update

The flow of streams toward rivers and rivers toward the sea is along a straight line, which connects them. The length of the line is a randomly chosen distance Z, which is given in Equation (18).

$$Z \epsilon \ (0, C \times d) \tag{18}$$

where C ranges between [1, 2] and it is usually taken as 2. The value of C being greater than unity makes the streams able to flow toward rivers in different directions. d is the current distance between the river and stream. Based on the above principle of flow, the updated positions of streams are given by Equation (19).

$$S^{j+1} = S^j \ + \ rand \times C \times (R^j - S^j) \tag{19}$$

where S^j and S^{j+1} are the current and updated positions of the stream, respectively. R^j is the position of river at j-th iteration. The updated position of the river is given by Equation (20) as

$$R^{j+1} \ = \ R^j \ + \ rand \times C \times (Sea^j - R^j) \tag{20}$$

where R^j and R^{j+1} are the current and updated positions of the river, respectively. Sea^j represents the position of the sea.

3.5. Evaporation Condition

The condition of evaporation helps to prevent becoming trapped in the local optima. If the distance between sea and river is less than a pre-defined value d_{max}, the process of rain starts. d_{max} is a small number close to zero. Its impact on the global optimal search is that the large value of d_{max} hinders the search, while its small value encourages the search closer to the sea [34]. Its value successively decreases after each iteration. The raining process occurs after evaporation.

3.6. Formation of New Streams

The locations of the newly formed streams are given by Equation (21).

$$S_{new} \ = \ LB \ + \ rand \times (UB - LB) \tag{21}$$

where S_{new} is the position of new streams, which directly flow to the sea. Equation (22) is used to generate streams whose flow is aimed directly toward the sea. This enhances the exploration near the optimal point in the feasible region for constrained problems.

$$S^{new} \ = \ Sea \ + \ \sqrt{v} \times randn(1, N_{var}) \tag{22}$$

where v shows the searching region range near the optimal point. In the majority of cases, the value of v is taken to be 0.1.

4. Simulation Setup

WCA is used to solve the fitness function to find the optimal switching angles such that the 5th and 7th harmonics are eliminated while the fundamental frequency is kept to a fixed value. MATLAB is used to implement WCA for SHE in a PC with Intel (R) Core™, i7, 2.7 GHz CPU and 8.00 GB RAM. Solutions obtained through WCA are compared with those obtained using PSO and FA. Parameters such as population size, number of iterations, and number of runs are kept same for the three algorithms for comparison. The parameters used for these algorithms are listed in Table 1.

Matlab-Simulink is used to perform simulation for a 7-level CHBMLI. To observe the effects of optimized switching angles on the eliminated harmonics, FFT analysis is also performed. The maximum DC voltage is selected as 300 V. Figure 4 explains the working flow of WCA with CHBMLI.

Table 1. Algorithm parameters.

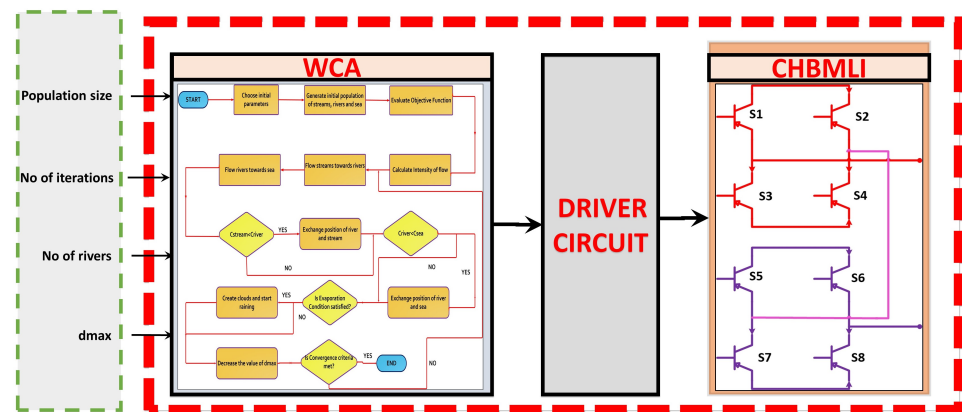| Algorithm	Parameter	
WCA	Population size	20
	Iterations	100
	Number of Rivers	4
	d_{max}	0.001
	Number of Runs	50
PSO	Population Size	20
	Iterations	100
	c1,c2	2
	Number of Runs	50
FA	Population Size	20
	Iterations	100
	Attractiveness Co-efficient	1
	Randomization parameter	0.5
	Absorption Co-efficient	1
	Number of Runs	50

Figure 4. Working flow of water cycle algorithm with CHBMLI.

The phase and line voltage waveforms obtained corresponding to modulation index 0.8 are shown in Figure 5. FFT analysis is than performed in SIMULINK to determine the percentages of eliminated harmonics with respect to fundamental. Figure 6 shows the result of the FFT analysis of the line voltage corresponding to a modulation index of 0.8.
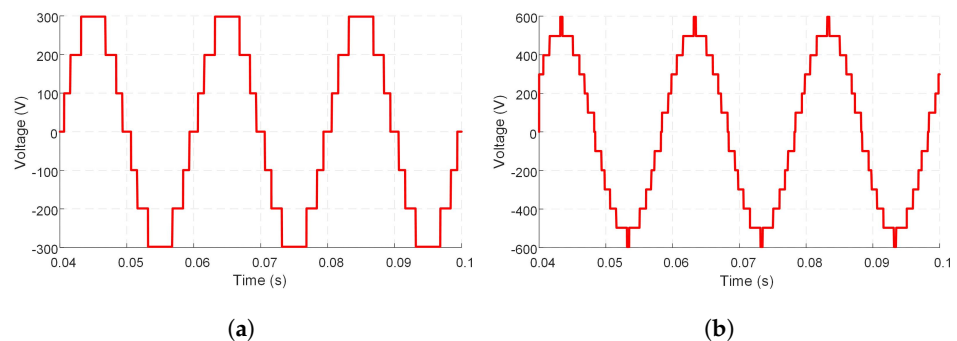

(a)

(b)

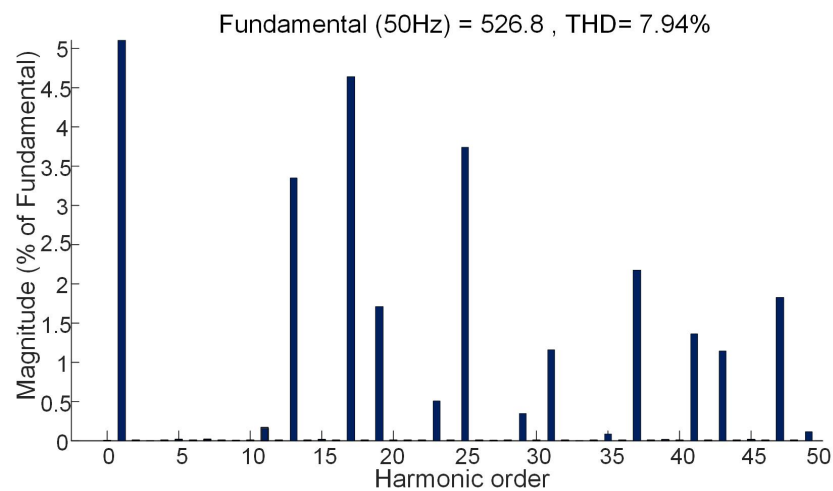**Figure 5.** (a) Phase voltage and (b) line voltage for m_a = 0.8.

Figure 6. FFT Analysis.

5. Results and Analysis

This section presents results and analysis on the selection of the switching angles, analysis of the percentage of the eliminated harmonics, and the convergence behavior of the algorithms while finding the solution. Moreover, due to the stochastic nature of the meta-heuristic optimization algorithms, different statistical tests are suggested to compare the performance of each algorithm statistically over a defined sample set. Figure 7 shows optimal switching angles obtained using WCA against different values of modulation index. From the given figure, it is evident that the value of the optimum solution set, comprising different switching angles, converges to a lower value with the increase in the value of the modulation index. ψ_1, ψ_2, and ψ_3 represent the switching angles at different values of the modulation index. Figure 8 shows the percentages of eliminated harmonics with respect to the fundamental against different values of the modulation index. From the given bar graph, it is clear that WCA outperforms PSO and FA by giving lower values of the harmonic percentage for CHBMLI. Moreover, the performance of FA and PSO is comparable, giving optimal results at different values of the modulation index. It is also obvious that the percentage of the 5th harmonic at different values of the modulation index dominates the 7th harmonic content in the overall harmonics percentage.
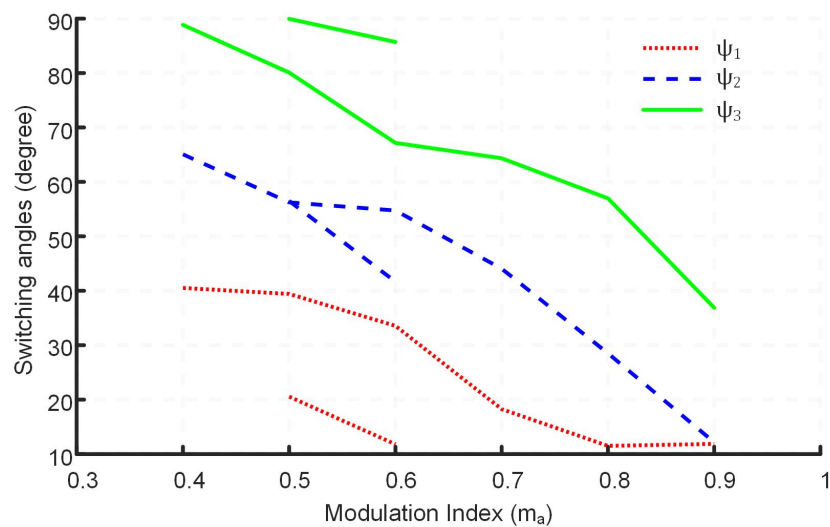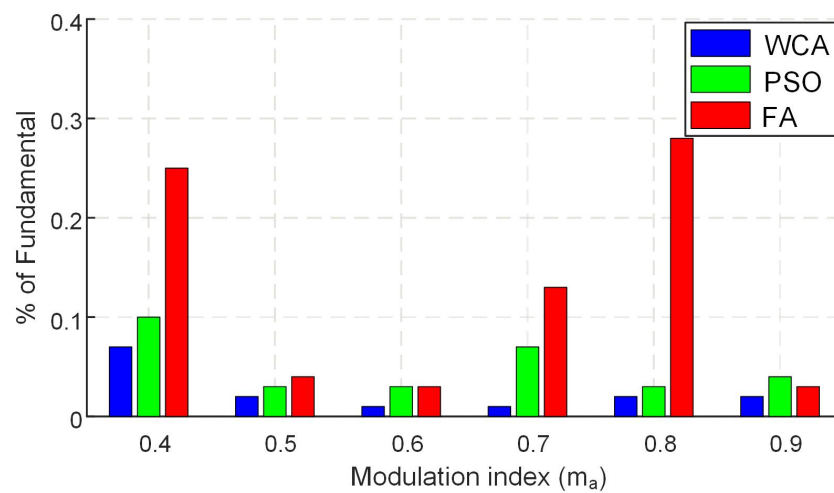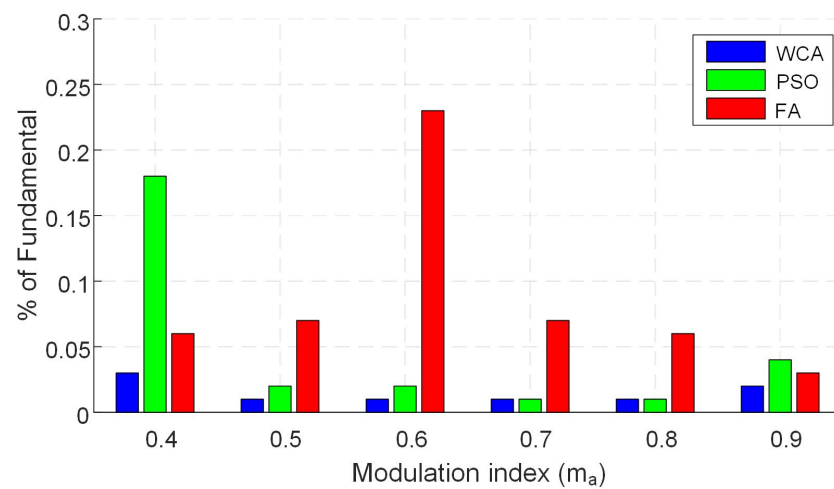

Figure 7. Switching angles for different values of modulation index.

(a)

(b)

Figure 8. Percentages of eliminated harmonics against each modulation index (m_a). (**a**) Contribution of 5th harmonic, (**b**) contribution of 7th harmonic.

5.1. Convergence Analysis

In order to obtain the convergence characteristic comparison, each meta-heuristic optimization algorithm is tested at different values of the modulation index. Further, the total number of iterations is kept at 100 for each algorithm, and the population size used is selected as 50 particles/fireflies or rain drops. Figures 9–14 show the results of the fitness value comparison of different algorithms against the modulation index values. From the given graphs, it can be observed that WCA outperforms the remaining algorithms by giving a lower fitness value. Moreover, WCA also converges to an optimal solution in fewer iterations. FA tends to become trapped in the local optima as the value of the modulation index increases.
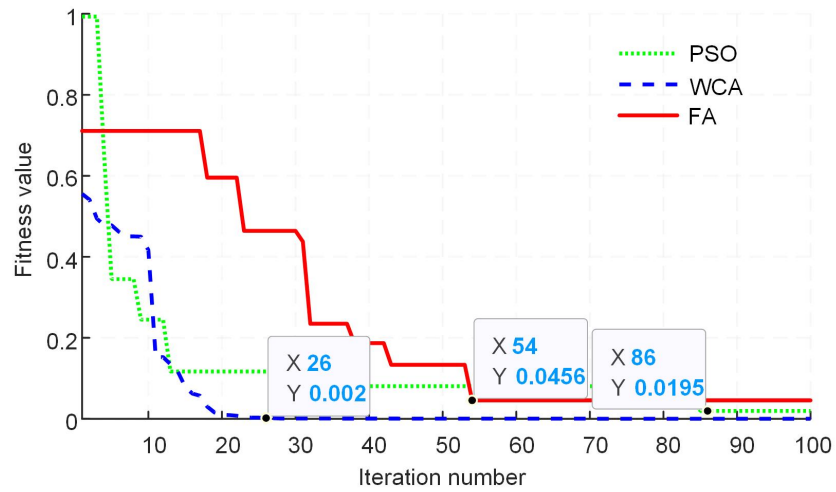
Figure 9. Fitness value comparison of different algorithms for modulation index value of 0.4.
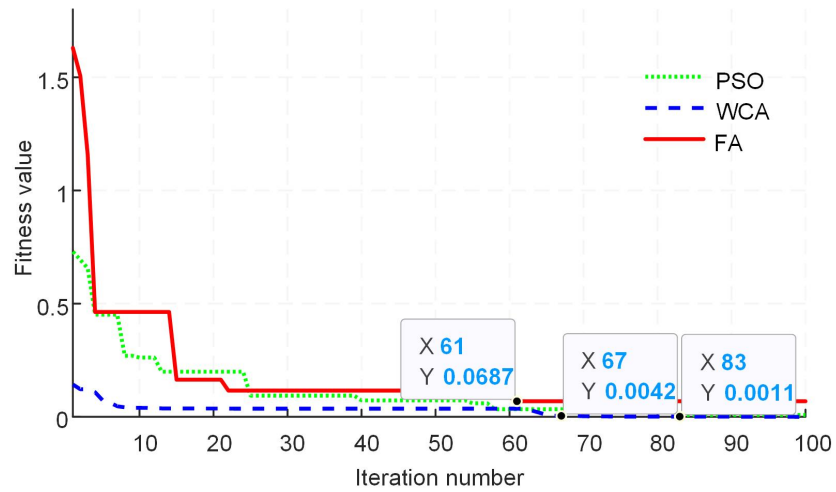

Figure 10. Fitness value comparison of different algorithms for modulation index value of 0.5.

Figure 11. Fitness value comparison of different algorithms for modulation index value of 0.6.

Figure 12. Fitness value comparison of different algorithms for modulation index value of 0.7.

Figure 13. Fitness value comparison of different algorithms for modulation index value of 0.8.

Figure 14. Fitness value comparison of different algorithms for modulation index value of 0.9.
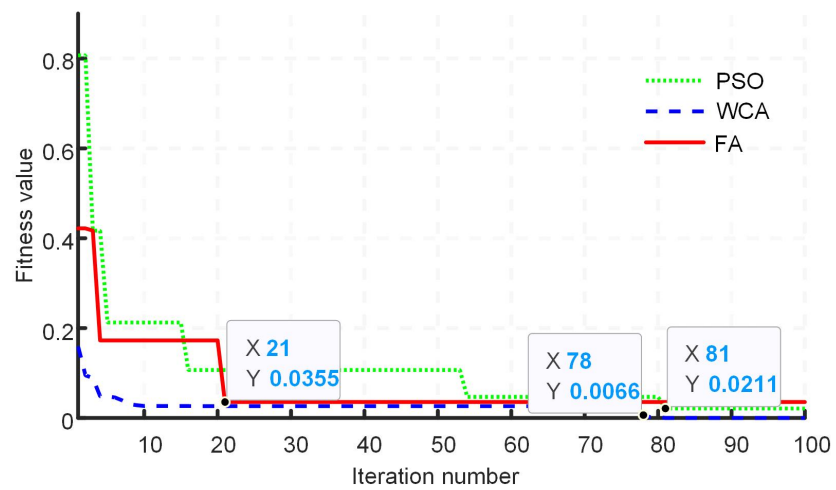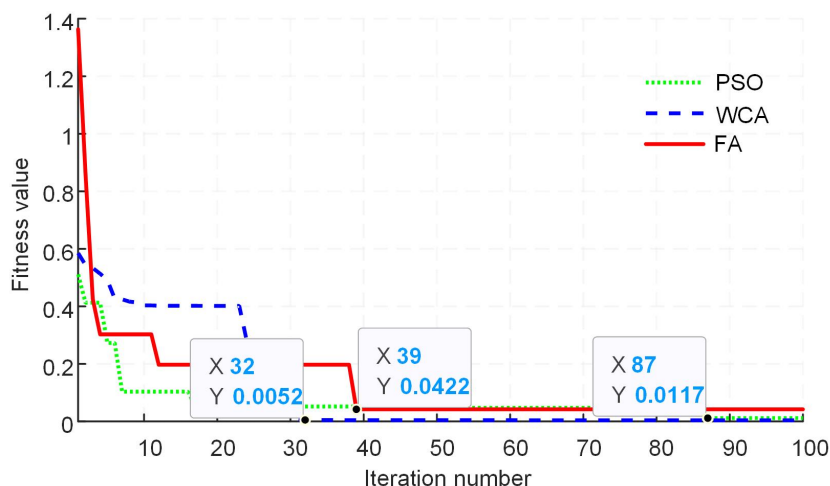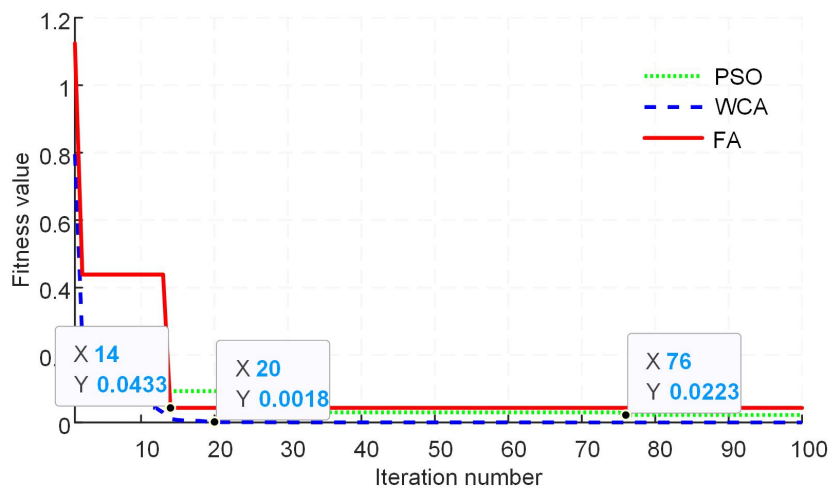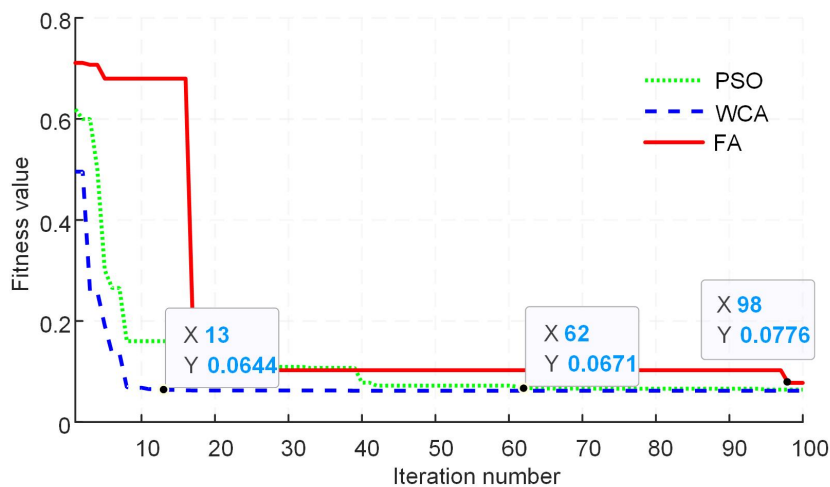
5.2. Fitness Values

The maximum, minimum and mean values obtained by the three algorithms for all modulation indexes for 50 runs are given in Table 2. It can be observed that the mean

value obtained by WCA for 50 samples over all modulation indexes is less as compared to PSO and FA.

Table 2. Maximum, minimum, and mean fitness values obtained by algorithms.

m_a	Algorithm	FF Value		
		Max	Min	Mean
	PSO	0.6728	0.014	0.1257
0.4	FA	0.3312	0.0361	0.1266
	WCA	0.298	2.08×10^{-5}	0.05
	PSO	0.37	0.013	0.081
0.5	FA	0.21	0.001	0.12
	WCA	0.35	0.001	0.06
	PSO	0.3316	0.012	0.08
0.6	FA	0.1703	0.03	0.1
	WCA	0.1867	0.0001	0.05
	PSO	0.4821	0.0219	0.1514
0.7	FA	0.3561	0.03	0.1506
	WCA	0.2618	0.0001	0.101
	PSO	0.5738	0.016	0.16
0.8	FA	0.6484	0.03	0.238
	WCA	0.3679	0.0001	0.0823
	PSO	0.8629	0.0676	0.1729
0.9	FA	0.8871	0.0761	0.2016
	WCA	0.4647	0.0558	0.0912

Figure 15 illustrates a graphical representation of the minimum, maximum and average fitness values obtained by the three algorithms for a modulation index of 0.8 over 50 samples. It is evident that the mean value obtained by WCA is less than that of PSO and FA over 50 samples. Moreover, the minimum value found by WCA over 50 samples is 0.0001, whereas those of PSO and FA are 0.0223 and 0.0433, which shows that WCA has better accuracy while finding the optimal solution.
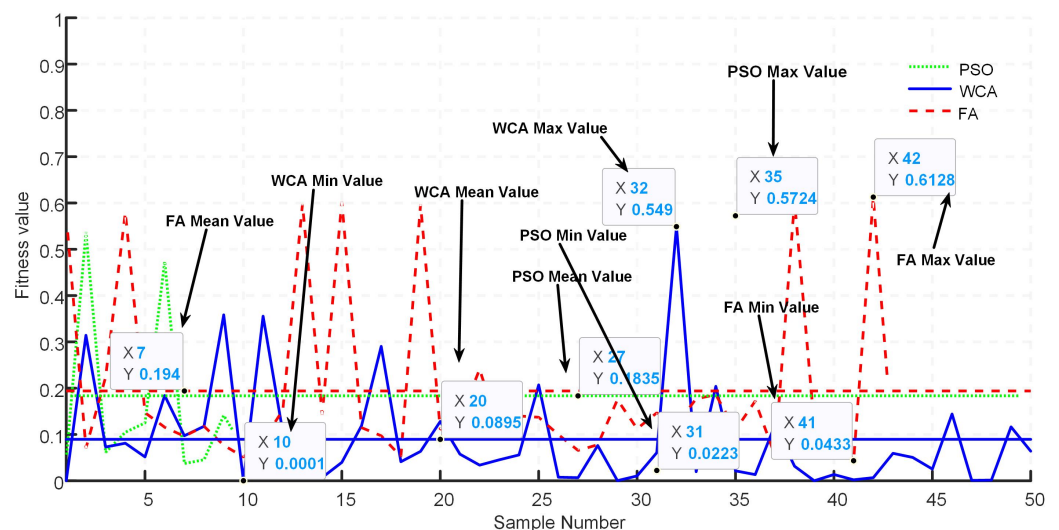
Figure 15. Fitness value for 50 runs.

5.3. Statistical Results

Meta-heuristic algorithms have a random nature. Due to this random nature, we obtain different results after each run. So, for comparing the performance of two metaheuristic algorithms, some statistics-based methods are used over a fixed sample size. In this research, we compare the average fitness value obtained by the algorithms for different population sizes, and to statistically differentiate them, we employ independent sample *t*-test results.

The independent sample *t*-test has two parts: one is Levene's test, which plays a role in the comparison of variances, and the second is the *t*-test, which is responsible for the comparison of means.

According to Levene's test and the *t*-test, for the results to be statistically different for the 95% confidence interval, the significant value should be smaller than the critical value of 0.05. In the case of the statistical comparison between PSO and WCA, we can see from Table 3 that for the population sizes of 20, 35 and 50, the significant values for both the *t*-test and Leven test of inequality, are less than 0.05, which means that the results obtained through WCA and PSO are statistically different for these population sizes. The execution time of WCA is more than that of PSO. In the case of FA and WCA, for a population size of 20, the *t*-test significant value is less than 0.05, so we can say that means are different, whereas variances are same. The same applies in the case for a population size of 35. It can be seen from Table 4 that the execution time of WCA is less than that of FA.

Table 3. Statistical comparison between WCA and PSO for 50 samples.

Size of Population	Avg. Fitness Value		Max Fitness Value		Min Fitness Value		Avg. Execution Time (Sec)		Sig. Values for Each Test	
	PSO	WCA	PSO	WCA	PSO	WCA	PSO	WCA	*t*-Test	Levene's Test
5	0.3341	0.4037	0.6835	0.8436	0.02	0.04	0.015	0.05	0.296	0.398
20	0.2233	0.1721	0.4537	0.549	0.033	0.0005	0.0451	0.1032	0.001	0.003
35	0.1196	0.0632	0.3789	0.1344	0.033	0.0003	0.0679	0.2817	0.004	0.006
50	0.1196	0.0411	0.3919	0.1199	0.02086	0.0002	0.124	0.3817	0.012	0.04

Table 4. Statistical comparison between WCA and FA for 50 samples.

Size of Population	Avg. Fitness Value		Max Fitness Value		Min Fitness Value		Avg. Execution Time (Sec)		Sig. Values	
	FA	WCA	FA	WCA	FA	WCA	FA	WCA	*t*-Test	Levene's Test
5	0.4500	0.4031	0.7538	0.8436	0.2101	0.0403	0.05	0.05	0.822	0.833
20	0.1204	0.1721	0.2028	0.549	0.07	0.3135	0.2049	0.1523	0.001	0.594
35	0.1026	0.0632	0.1560	0.1344	0.0548	0.0003	0.8251	0.2817	0.02	0.44
50	0.1707	0.0411	0.5919	0.1199	0.0589	0.0002	1.6473	0.3817	0.215	0.04

6. Conclusions

The water cycle algorithm is easy to implement, as it has only one tuning parameter as compared to particle swarm optimization and firefly algorithms. The water cycle algorithm gave competitive results compared to particle swam optimization and firefly algorithms for harmonic elimination in a seven-level cascaded H-bridge multi-level inverter. It also converges to the optimal solution in less number of iterations and its accuracy is better. The mean fitness value achieved by water cycle algorithm over 50 samples is less as compared to particle swarm optimization and firefly algorithms. For most of the population sizes, results obtained through water cycle algorithm are better from those obtained through particle swarm optimization and firefly algorithms. The drawback of WCA is the initial tuning and online tuning with faults, which needs to be further studied. In future, the application of water cycle algorithm can be applied for solving SHE equations for harmonic elimination in higher-level inverters.

Conflicts of Interest: The authors declare no conflict of interest.

Nomenclature

The following abbreviations and notations are used in this manuscript:

Abbreviations

CHBMLI	Cascaded H-Bridge Multilevel Inverter
EMI	Electromagnetic Interference
FA	Firefly Algorithm
MLI	Multilevel Inverter
PSO	Particle Swarm Optimization
RES	Renewable Energy Systems
SHE	Selective Harmonic Elimination
WCA	Water Cycle Algorithm
NR	Newton–Raphson
BA	Bee Algorithm
GA	Genetic Algorithm
CSA	Cuckoo Search Algorithm
BOA	Bat Optimization Algorithm
ACO	Ant Colony Optimization
GWO	Grey Wolf Optimizer
MGWO	Modified Grey Wolf Optimizer
SSA	Salt Swarm Algorithm

Notations

V_{dc}	DC Voltage applied to H–Bridge Cell
V_1	Fundamental component
FF	Fitness function
m_a	Modulation index
N_{pop}	Population size
N_{var}	Number of variables
nr	Number of rivers
N_s	Number of streams
N_{sr}	Sum of sea and rivers
NS_i	Number of streams allocated to particular sea or rivers
d	Current distance between stream and river
S^j	Current position of stream at j-th
S^{j+1}	Updated position of stream at $j + 1$ iteration
R^j	Current position of river at j-th
R^{j+1}	Updated position of river at $j + 1$ iteration
S_{new}	Position of new streams which directly flow towards sea
LB	Lower bound
UB	Upper bound

References

1. Ali, M.; Din, Z.; Solomin, E.; Cheema, K.M.; Milyani, A.H.; Che, Z. Open switch fault diagnosis of cascade H-bridge multi-level inverter in distributed power generators by machine learning algorithms. *Energy Rep.* **2021**, *7*, 8929–8942. [CrossRef]
2. Flourentzou, N.; Agelidis, V.G.; Demetriades, G.D. VSC-based HVDC power transmission systems: An overview. *IEEE Trans. Power Electron.* **2009**, *24*, 592–602. [CrossRef]
3. Song, Q.; Liu, W. Control of a cascade STATCOM with star configuration under unbalanced conditions. *IEEE Trans. Power Electron.* **2009**, *24*, 45–58. [CrossRef]
4. Sadigh, A.K.; Hosseini, S.H.; Sabahi, M.; Gharehpetian, G.B. Double flying capacitor multicell converter based on modified phase-shifted pulsewidth modulation. *IEEE Trans. Power Electron.* **2009**, *25*, 1517–1526. [CrossRef]
5. Hatti, N.; Hasegawa, K.; Akagi, H. A 6.6-kV transformerless motor drive using a five-level diode-clamped PWM inverter for energy savings of pumps and blowers. *IEEE Trans. Power Electron.* **2009**, *24*, 796–803. [CrossRef]
6. Nami, A.; Zare, F.; Ghosh, A.; Blaabjerg, F. A hybrid cascade converter topology with series-connected symmetrical and asymmetrical diode-clamped H-bridge cells. *IEEE Trans. Power Electron.* **2009**, *26*, 51–65. [CrossRef]
7. Kumar, P.; Kour, M.; Goyal, S.K.; Singh, B.P. Multilevel inverter topologies in renewable energy applications. In *Intelligent Computing Techniques for Smart Energy Systems*; Springer: Berlin/Heidelberg, Germany, 2020; pp. 891–902.

8. Benyamina, F.; Benrabah, A.; Khoucha, F.; Zia, M.F.; Achour, Y.; Benbouzid, M. An augmented state observer-based sensorless control of grid-connected inverters under grid faults. *Int. J. Electr. Power Energy Syst.* **2021**, *133*, 107222. [CrossRef]

9. Zia, M.; Elbouchikhi, E.; Benbouzid, M. An energy management system for hybrid energy sources-based stand-alone marine microgrid. In *IOP Conference Series: Earth and Environmental Science*; IOP Publishing: Bristol, UK, 2019; Volume 322, p. 012001.

10. Janardhan, K.; Mittal, A.; Ojha, A. Performance investigation of stand-alone solar photovoltaic system with single phase micro multilevel inverter. *Energy Rep.* **2020**, *6*, 2044–2055. [CrossRef]

11. Abbasi, M.A.; Zia, M.F. Novel TPPO based maximum power point method for photovoltaic system. *Adv. Electr. Comput. Eng.* **2017**, *17*, 95–100. [CrossRef]

12. Memon, M.A.; Mekhilef, S.; Mubin, M.; Aamir, M. Selective harmonic elimination in inverters using bio-inspired intelligent algorithms for renewable energy conversion applications: A review. *Renew. Sustain. Energy Rev.* **2018**, *82*, 2235–2253. [CrossRef]

13. Liang, T.J.; O'Connell, R.M.; Hoft, R.G. Inverter harmonic reduction using Walsh function harmonic elimination method. *IEEE Trans. Power Electron.* **1997**, *12*, 971–982. [CrossRef]

14. Aghdam, G.H. Optimised active harmonic elimination technique for three-level T-type inverters. *IET Power Electron.* **2013**, *6*, 425–433. [CrossRef]

15. Kumar, J.; Das, B.; Agarwal, P. Harmonic reduction technique for a cascade multilevel inverter. *Int. J. Recent Trends Eng.* **2009**, *1*, 181.

16. Sun, J.; Grotstollen, H. Solving nonlinear equations for selective harmonic eliminated PWM using predicted initial values. In Proceedings of the 1992 International Conference on Industrial Electronics, Control, Instrumentation, and Automation, San Diego, CA, USA, 13 November 1992; pp. 259–264.

17. Imarazene, K.; Chekireb, H. Selective harmonics elimination PWM with self-balancing DC-link in photovoltaic 7-level inverter. *Turk. J. Electr. Eng. Comput. Sci.* **2016**, *24*, 3999–4014. [CrossRef]

18. Yang, K.; Zhang, Q.; Yuan, R.; Yu, W.; Yuan, J.; Wang, J. Selective harmonic elimination with Groebner bases and symmetric polynomials. *IEEE Trans. Power Electron.* **2015**, *31*, 2742–2752. [CrossRef]

19. Zheng, C.; Zhang, B. Application of Wu method to harmonic elimination techniques. *Proc. CSEE* **2005**, *25*, 40–45.

20. Chiasson, J.N.; Tolbert, L.M.; McKenzie, K.J.; Du, Z. Elimination of harmonics in a multilevel converter using the theory of symmetric polynomials and resultants. *IEEE Trans. Control. Syst. Technol.* **2005**, *13*, 216–223. [CrossRef]

21. Chiasson, J.N.; Tolbert, L.M.; Du, Z.; McKenzie, K.J. The use of power sums to solve the harmonic elimination equations for multilevel converters. *EPE J.* **2005**, *15*, 19–27. [CrossRef]

22. Al-Othman, A.; Ahmed, N.A.; AlSharidah, M.; AlMekhaizim, H.A. A hybrid real coded genetic algorithm–pattern search approach for selective harmonic elimination of PWM AC/AC voltage controller. *Int. J. Electr. Power Energy Syst.* **2013**, *44*, 123–133. [CrossRef]

23. Reza Salehithe, R.; Farokhnia, N.; Abedi, M.; Fathi, S. Elimination of low order harmonics in multilevel inverters using genetic algorithm. *J. Power Electron.* **2011**, *11*, 132–139.

24. Shen, K.; Zhao, D.; Mei, J.; Tolbert, L.M.; Wang, J.; Ban, M.; Ji, Y.; Cai, X. Elimination of harmonics in a modular multilevel converter using particle swarm optimization-based staircase modulation strategy. *IEEE Trans. Ind. Electron.* **2014**, *61*, 5311–5322. [CrossRef]

25. Kavousi, A.; Vahidi, B.; Salehi, R.; Bakhshizadeh, M.K.; Farokhnia, N.; Fathi, S.H. Application of the bee algorithm for selective harmonic elimination strategy in multilevel inverters. *IEEE Trans. Power Electron.* **2011**, *27*, 1689–1696. [CrossRef]

26. Ajami, A.; Mohammadzadeh, B.; Oskuee, M.R.J. Utilizing the cuckoo optimization algorithm for selective harmonic elimination strategy in the cascaded multilevel inverter. *ECTI Trans. Electr. Eng. Electron. Commun.* **2014**, *12*, 7–15.

27. Ganesan, K.; Barathi, K.; Chandrasekar, P.; Balaji, D. Selective harmonic elimination of cascaded multilevel inverter using BAT algorithm. *Procedia Technol.* **2015**, *21*, 651–657. [CrossRef]

28. Karthik, N.; Arul, R. Harmonic elimination in cascade multilevel inverters using Firefly algorithm. In Proceedings of the 2014 International Conference on Circuits, Power and Computing Technologies (ICCPCT-2014), Nagercoil, India, 20–21 March 2014; pp. 838–843.

29. Babaei, M.; Rastegar, H. Selective harmonic elimination PWM using ant colony optimization. In Proceedings of the 2017 Iranian Conference on Electrical Engineering (ICEE), Tehran, Iran, 2–4 May 2017; pp. 1054–1059.

30. Dzung, P.Q.; Tien, N.T.; Tuyen, N.D.; Lee, H.H. Selective harmonic elimination for cascaded multilevel inverters using grey wolf optimizer algorithm. In Proceedings of the 2015 9th International Conference on Power Electronics and ECCE Asia (ICPE-ECCE Asia), Seoul, Korea, 1–5 June 2015; pp. 2776–2781.

31. Routray, A.; Singh, R.K.; Mahanty, R. Harmonic reduction in hybrid cascaded multilevel inverter using modified grey wolf optimization. *IEEE Trans. Ind. Appl.* **2019**, *56*, 1827–1838. [CrossRef]

32. Babu, T.S.; Priya, K.; Maheswaran, D.; Kumar, K.S.; Rajasekar, N. Selective voltage harmonic elimination in PWM inverter using bacterial foraging algorithm. *Swarm Evol. Comput.* **2015**, *20*, 74–81. [CrossRef]

33. Hosseinpour, M.; Mansoori, S.; Shayeghi, H. Selective Harmonics Elimination Technique in Cascaded H-Bridge Multi-Level Inverters Using the Salp Swarm Optimization Algorithm. *J. Oper. Autom. Power Eng.* **2020**, *8*, 32–42.

34. Eskandar, H.; Sadollah, A.; Bahreininejad, A.; Hamdi, M. Water cycle algorithm—A novel metaheuristic optimization method for solving constrained engineering optimization problems. *Comput. Struct.* **2012**, *110*, 151–166. [CrossRef]